PROCEEDINGS OF SCIENCE

TeV Scale Leptogenesis via Dark Sector

Sin Kyu Kang*
School of Liberal Arts, Seoul-Tech, Seoul 139-743, Korea
E-mail: skkang@seoultech.ac.kr

Debasish Borah
Department of Physics, Indian Institute of Technology Guwahati, Assam 781039, India
E-mail: dborah@iitg.ac.in

Arnab Dasgupta
School of Liberal Arts, Seoul-Tech, Seoul 139-743, Korea
E-mail: arnabdasgupta@protonmail.ch

We study the possibility of realising successful leptogenesis from dark matter annihilations in the scotogenic model of neutrino masses to explain the same order of magnitude abundance of dark matter and baryons in the present Universe, and show that the correct leptonic asymmetry, dark matter abundance and neutrino mass can be simultaneously achieved in the model. Interestingly, the scale of leptogenesis can be as low as 5 TeV, lower than the one in vanilla leptogenesis scenario in scotogenic model along with the additional advantage of explaining the baryon-dark matter coincidence. Due to such low scale, the model remains predictive at dark matter direct detection and rare decay experiments looking for charged lepton flavour violating processes

Corfu Summer Institute 2019 "School and Workshops on Elementary Particle Physics and Gravity" (CORFU2019)
31 August - 25 September 2019
Corfù, Greece

*Speaker.

PoS(CORFU2019)034

1. Introduction

There have been significant progress in last few decades in gathering evidences suggesting the presence of a mysterious, non-luminous form of matter, known as dark matter (DM) in the present Universe, whose amount is approximately five times more than the ordinary luminous or baryonic matter density $\Omega_B \approx 5\%$ [1]. Among different beyond standard model (BSM) proposals for DM, the weakly interacting massive particle (WIMP) paradigm remains the most widely studied scenario where a DM candidate typically with electroweak (EW) scale mass and interaction rate similar to EW interactions can give rise to the correct DM relic abundance, a remarkable coincidence often referred to as the *WIMP Miracle*. On the other hand, out of equilibrium decay of a heavy particle leading to the generation of baryon asymmetry has been a very well known mechanism for baryogenesis [2, 3]. One interesting way to implement such a mechanism is leptogenesis [4] where a net leptonic asymmetry is generated first which gets converted into baryon asymmetry through $B+L$ violating EW sphaleron transitions. The interesting feature of this scenario is that the required lepton asymmetry can be generated within the framework of the seesaw mechanism that explains the origin of tiny neutrino masses [5], another observed phenomena which the SM fails to address.

Although these popular scenarios can explain the phenomena of DM and baryon asymmetry independently, it is nevertheless an interesting observation that DM and baryon abundance are very close to each other, within the same order of magnitudes $\Omega_{\rm DM} \approx 5\Omega_B$. Discarding the possibility of any numerical coincidence, one is left with the task of constructing theories that can relate the origin of these two observed phenomena in a unified manner. There have been several proposals already which mainly fall into two broad categories. In the first one, the usual mechanism for baryogenesis is extended to apply to the dark sector which is also asymmetric [6, 7, 8, 9]. The second one is to produce such asymmetries through annihilations [10, 10, 11, 12] where one or more particles involved in the annihilations eventually go out of thermal equilibrium in order to generate a net asymmetry. The so-called WIMPy baryogenesis [13, 14, 15] belongs to this category, where a dark matter particle freezes out to generate its own relic abundance and then an asymmetry in the baryon sector is produced from DM annihilations. The idea extended to leptogenesis is called WIMPy leptogenesis [16, 17, 18].

While there is no evidence yet for seesaw mechanism, recently the so-called scotogenic model [19] as an alternative to canonical seesaw mechanism has been extensively studied, where Majorana light neutrino masses can be generated at one loop level with DM particle in the loop. In the scotogenic model, the required lepton asymmetry can be generated through right handed neutrino decays [20, 21] at a low scale $M_N \sim 10$ TeV at the cost of a strongly hierarchical neutrino Yukawa structure, but it can not explain the coincidence of baryon asymmetry and DM abundance. Then, an interesting question raised is whether WIMPy leptogenesis can be realised remedying the weak points in vanilla leptogenesis in the scotogenic model. Giving the answer to this question is the main purpose of this work. We examine how the DM annihilation can produce the lepton asymmetry while keeping the correct DM abundance so that the coincidence of their values can be naturally explained. Due to the absence of typical s-channel diagrams of DM annihilations leading to leptonic asymmetry, here we show how a t-channel diagram can play a non-trivial role in creating the required asymmetry. However, it will turn out that it is hard to satisfy the requirements

PoS(CORFU2019)034

for DM, baryon asymmetry and neutrino mass simultaneously in the minimal scotogenic model. To successfully realise the WIMPy leptogenesis, we minimally extend the scotogenic model by adding a singlet scalar field where all such requirements can be fulfilled while keeping the scale of leptogenesis as low as 5 TeV, lower than the scale of vanilla leptogenesis [21]. Due to such a low scale, the model has another advantage to predict observable rates of charged lepton flavour violation accessible by the sensitivity of the future experiments.

2. Minimal Scotogenic Model

The minimal scotogenic model [19] is the extension of the SM by three copies of right handed singlet neutrinos $N_i, i \in 1,2,3$ and one scalar field η transforming as a doublet under $SU(2)_L$. An additional discrete symmetry Z_2 is incorporated under which these new fields are odd giving rise to the possibility of the lightest Z_2-odd particle being a suitable DM candidate. The Lagrangian involving the newly added singlet fermions is

$$\mathscr{L} \supset \frac{1}{2}(M_N)_{ij}N_iN_j + (Y_{ij}\bar{L}_i\tilde{\eta}N_j + h.c.) \ . \tag{2.1}$$

The electroweak symmetry breaking occurs due to the non-zero vacuum expectation value (VEV) acquired by the neutral component of the SM Higgs doublet while the Z_2-odd doublet η does not acquire any VEV. After the EWSB these two scalar doublets can be written in the following form in the unitary gauge,

$$H = \left(0, \ \frac{v+h}{\sqrt{2}}\right)^T, \quad \eta = \left(\eta^{\pm}, \ \frac{\eta_R + i\eta_I}{\sqrt{2}}\right)^T. \tag{2.2}$$

The scalar potential of the model is

$$V = \mu_H^2|H|^2 + \mu_\eta^2|\eta|^2 + \frac{\lambda_1}{2}|H|^4 + \frac{\lambda_2}{2}|\eta|^4 + \lambda_3|H|^2|\eta|^2 + \lambda_4|H^\dagger\eta|^2 + \{\frac{\lambda_5}{2}(H^\dagger\eta)^2 + h.c.\} \tag{2.3}$$

The masses of the physical scalars at tree level can be written as

$$\begin{aligned} m_h^2 &= \lambda_1 v^2, \quad m_{\eta^\pm}^2 = \mu_2^2 + \frac{1}{2}\lambda_3 v^2, \\ m_{\eta_R}^2 &= \mu_2^2 + \frac{1}{2}(\lambda_3+\lambda_4+\lambda_5)v^2 = m_{H^\pm}^2 + \frac{1}{2}(\lambda_4+\lambda_5)v^2, \\ m_{\eta_I}^2 &= \mu_2^2 + \frac{1}{2}(\lambda_3+\lambda_4-\lambda_5)v^2 = m_{H^\pm}^2 + \frac{1}{2}(\lambda_4-\lambda_5)v^2. \end{aligned} \tag{2.4}$$

Here m_h is the SM like Higgs boson mass, m_{η_R}, m_{η_I} are the masses of the CP even and CP odd scalars from the inert doublet. $m_{\eta^\pm}$ is the mass of the charged scalar. Without any loss of generality, we consider $\lambda_5 < 0, \lambda_4+\lambda_5 < 0$ so that the CP even scalar is the lightest Z_2 odd particle and hence a stable dark matter candidate.

Denoting the squared physical masses of neutral scalar and pseudo-scalar parts of η as $m_{R,I}^2 = m_{\eta_R,\eta_I}^2$ and the mass of the right handed neutrino N_k in the internal line as M_k, the one loop neutrino mass can be estimated as [19]

$$(M_\nu)_{ij} = \sum_k \frac{Y_{ik}Y_{jk}M_k}{32\pi^2}\left[L_k(m_{\eta_R}^2) - L_k(m_{\eta_I}^2)\right] , \tag{2.5}$$

where M_k is the mass eigenvalue of the right handed neutrino mass eigenstate N_k in the internal line and the indices $i, j = 1,2,3$ run over the three neutrino generations as well as three copies of N_i. The function $L_k(m^2)$ is defined as $L_k(m^2) = \frac{m^2}{m^2-M_k^2} \ln \frac{m^2}{M_k^2}$. From the physical scalar masses given above, we note that $m^2_{\eta_R} - m^2_{\eta_I} = \lambda_5 v^2$. In this model for the neutrino mass to match with experimentally observed limits (~ 0.1 eV), Yukawa couplings of the order 10^{-3} are required if M_k is as low as 1 TeV and the mass difference between η_R and η_I is kept around 1 GeV. Such a small mass splitting between η_R and η_I will correspond to small quartic coupling $\lambda_5 \sim 10^{-4}$. Thus, one can suitably choose the Yukawa couplings, quartic coupling λ_5 and M_k in order to arrive at sub eV light neutrino masses. The light neutrino mass matrix is diagonalised by the usual PMNS mixing matrix U, which is determined from the neutrino oscillation data (up to the Majorana phases):

$$D_\nu = U^\dagger M_\nu U^* = \mathrm{diag}(m_1, m_2, m_3)\,. \tag{2.6}$$

Then the Yukawa coupling matrix satisfying the neutrino data can be written as [22] $Y = U D_\nu^{1/2} O \widetilde{M}^{1/2}$, where O is an arbitrary complex orthogonal matrix.

Here we consider η_R as the DM candidate ($\eta_R \equiv$ DM) which is similar to the inert doublet model discussed extensively in the literature [19, 23, 24]. Typically there exists two distinct mass regions, $M_{\rm DM} \leq 80$ GeV and $M_{\rm DM} \geq 500$ GeV, where correct relic abundance criteria can be satisfied. In both regions, depending on the mass differences $m_{\eta^\pm} - m_{\eta_R}, m_{\eta_I} - m_{\eta_R}$, the coannihilations of $\eta_R, \eta^\pm$ and η_R, η_I can also contribute to the DM relic abundance [25, 26].

3. Leptogenesis from annihilations

In the minimal scotogenic model discussed in the previous section, there are different types of annihilation processes which violate lepton number. They are namely,

1. annihilation process of scalar doublet η: $\eta\eta \to L_\alpha L_\beta$.
2. coannihilation process of scalar doublet and one of the singlet fermions: $\eta N \to LX$ where ($X \equiv h, \gamma, W^\pm, Z$).

Interestingly, if we put the additional constraints that such lepton number violating annihilations and coannihilations also generate a non-zero CP asymmetry, they lead to two different DM possibilities namely,

1. the lightest neutral component of inert scalar doublet η as DM,
2. the lightest right handed neutrino N as DM.

The Boltzmann equations for leptonic asymmetry is given as follows:

$$
\begin{aligned}
\frac{dY_{\Delta L}}{dz} &= \frac{1}{zH(z)}\Bigg[\sum_i \varepsilon_{N_i}(Y_{N_i}-Y_{N_i}^{\rm eq})\langle\Gamma_{N_i\to L_\alpha\eta}\rangle - Y_{\Delta L} r_{N_i}\langle\Gamma_{N_i\to L_\alpha\eta}\rangle - Y_{\Delta L} r_\eta s\langle\Gamma_{\eta\to N_1 L}\rangle \\
&+2\varepsilon_{\eta\eta} s\langle\sigma v\rangle_{\eta\eta\to LL}\left(Y_\eta^2-(Y_\eta^{\rm eq})^2\right) - Y_{\Delta L} Y_L^{\rm eq} r_\eta^2 s\langle\sigma v\rangle_{\eta\eta\to LL} \\
&+\sum_i \varepsilon_{N_i\eta} s\langle\sigma v\rangle_{\eta N_i\to L{\rm SM}}\left(Y_\eta Y_{N_i}-Y_\eta^{\rm eq}Y_{N_i}^{\rm eq}\right) - \frac{1}{2} Y_{\Delta L} Y_L^{\rm eq} r_{N_i} r_\eta s\langle\sigma v\rangle_{\eta N_i\to {\rm SM}\bar{L}} \\
&-Y_{\Delta L} Y_\eta^{\rm eq} s\langle\sigma v\rangle^{wo}_{\eta L\to\eta\bar{L}} - \sum_i Y_{\Delta L} Y_\eta^{\rm eq} s\langle\sigma v\rangle^{wo}_{\eta L\to N_i X} - \sum_i Y_{\Delta L} Y_{N_i}^{\rm eq} s\langle\sigma v\rangle^{wo}_{N_i L\to\eta X}\Bigg], \qquad (3.1) \\
H(z) &= \sqrt{\frac{4\pi^3 g_*}{45}}\frac{M_{\rm DM}^2}{z^2 M_{\rm PL}}, \qquad s = g_*\frac{2\pi^2}{45}\left(\frac{M_{\rm DM}}{z}\right)^3, \\
r_j &= \frac{Y_j^{\rm eq}}{Y_L^{\rm eq}}, \qquad \langle\Gamma_{j\to X}\rangle = \frac{K_1(M_j/T)}{K_2(M_j/T)}\Gamma_{j\to X},
\end{aligned}
$$

where $z = \frac{M_{\rm DM}}{T}$, $M_{\rm PL}$ is the Planck mass and $Y = n/s$ denotes the comoving number density, as the ratio of number density to entropy density. The details of the derivation of this Boltzmann equation as well as the relevant equations for DM are presented in appendix of Ref.[27]. In the above equation, $\varepsilon_{\eta\eta}$ and $\varepsilon_{N_i\eta}$ will be given appropriately later and ε_{N_i} is shown in [21]. M_{DM} in s is the mass of Z_2 odd particle taken appropriately depending on the scenario mentioned above. Here K_n is the nth order Modified Bessel function of second kind.

We present tree and all such 1-loop diagrams contributing to the asymmetry arising from the interference at order $\mathscr{O}(y^4g^2)$ and $\mathscr{O}(y^6)$ in Fig. 1 and Fig. 2. Similarly, there exists several washout processes that can be constructed by swapping initial and final state particles. This is true for fermion dark matter as well, which we discuss in one of the upcoming sections.

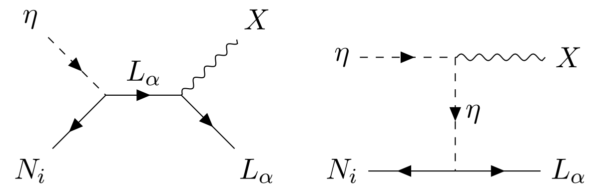

Figure 1: Feynman diagrams contributing to $\langle\sigma v\rangle_{{\rm DMDM}\to XL}$ and the asymmetry ε at leading order. Here $X \equiv \gamma, W^\pm, Z$.

3.1 Scalar doublet η as Dark Matter

In this scenario the only way to get asymmetry is through co-annihilations. Pure scalar annihilations give rise to vanishing leptonic asymmetry if η is the lightest Z_2 odd particle, as required for it to be the DM candidate. This is particularly due to the fact the "on-shell" criteria of loop particles can not be realised in such case, resulting in a vanishing CP asymmetry, as we discuss below. For

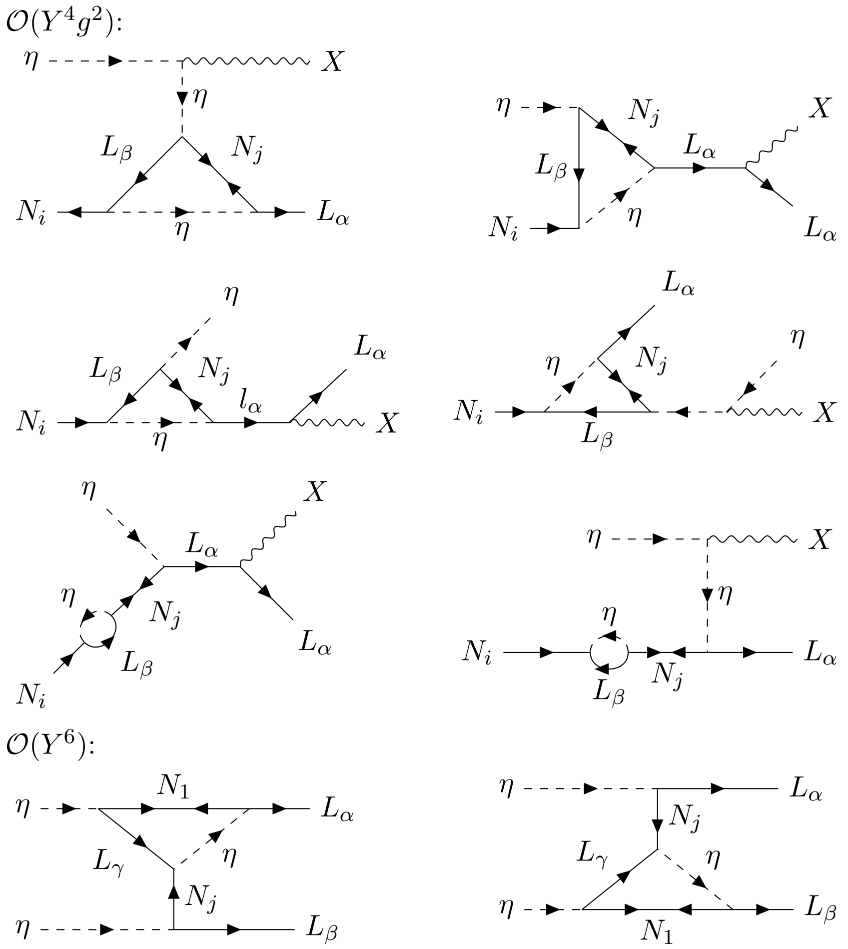

Figure 2: 1-loop diagrams contributing to the asymmetry arising from the interference at $\mathscr{O}(y^4g^2)$ and $\mathscr{O}(y^6)$.

this scenario the Boltzmann equations for the Z_2 odd particles take the following form:

$$\begin{aligned}
\frac{dY_{N_k}}{dz} &= -\tfrac{1}{zH(z)}\Big[(Y_{N_k}-Y_{N_k}^{\rm eq})\langle\Gamma_{N_k\to L_\alpha\eta}\rangle + (Y_{N_k}Y_\eta - Y_{N_k}^{\rm eq}Y_\eta^{\rm eq})s\langle\sigma v\rangle_{\eta N_k\to L{\rm SM}} \\
&\qquad + \textstyle\sum_{l=1}^{3}(Y_{N_k}Y_{N_l}-Y_{N_k}^{\rm eq}Y_{N_l}^{\rm eq})s\langle\sigma v\rangle_{N_lN_k\to{\rm SMSM}}\Big], \\
\frac{dY_\eta}{dz} &= \tfrac{1}{zH(z)}\Big[(Y_{N_k}-Y_{N_k}^{\rm eq})\langle\Gamma_{N_i\to L_\alpha\eta}\rangle - 2(Y_\eta^2-(Y_\eta^{\rm eq})^2)s\langle\sigma v\rangle_{\eta\eta\to{\rm SMSM}} \\
&\qquad - \textstyle\sum_{m=1}^{3}(Y_{N_m}Y_\eta - Y_{N_m}^{\rm eq}Y_\eta^{\rm eq})s\langle\sigma v\rangle_{\eta N_m\to L{\rm SM}}\Big].
\end{aligned} \tag{3.2}$$

The CP asymmetry arising from the interference between tree and 1-loop diagrams in Fig. 1

and Fig. 2 can be estimated as

$$\varepsilon_{N_i\eta} = \frac{2}{(yy^\dagger)_{ii}}\sum_j \Im[(yy^\dagger)^2_{ij}]\widetilde{\varepsilon}_{ij}, \tag{3.3}$$

$$\begin{aligned}
\widetilde{\varepsilon}_{ij} =& \frac{\sqrt{x_j}}{6x_i\left(-x_i^{3/2}+x_i(x_j-2)+\sqrt{x_i}x_j+1\right)^2(\sqrt{x_i}-3)}\left(x_i^{7/2}(3x_j+1)+\sqrt{x_i}(3x_j+5)+1\right.\\
&-3x_i^{5/2}\left(x_j\left(D+(x_j-3)x_j+4\right)-3D-2\right)-3x_i^{3/2}\left(2\left(D+3\right)+x_j\left(x_j\left(D+x_j+1\right)-D-4\right)\right)\\
&\left.-x_i^4+f^3\left(3D+3x_j^2+11\right)-3x_i^2\left(x_j\left(D+2(x_j-1)x_j+2\right)-D+6\right)+x_i\left(1-3x_j\left(D+x_j-4\right)\right)\right)\\
&+\frac{\sqrt{x_j}}{4x_i}\left(\sqrt{x_i}-1+\frac{\sqrt{x_j}}{(1+\sqrt{x_i})^2}(\sqrt{x_i}-1+r_j)\left(\log\left(\frac{1+\sqrt{x_i}x_j}{x_i(1+\sqrt{x_i})}\right)-\log\left(\frac{1+x_i+x_i^{3/2}+\sqrt{x_i}x_j}{x_i(1+\sqrt{x_i})}\right)\right.\right.\\
&\left.\left.+\log\left(1+\frac{1+\sqrt{x_i}}{\sqrt{x_i}(\sqrt{x_i}-1+x_i+x_j)}\right)\right)\right)+\frac{\sqrt{x_i}x_j\tilde{\Gamma}_j}{\pi((x_i-x_j)^2+x_j\tilde{\Gamma}_j^2)}
\end{aligned} \tag{3.4}$$

$$D = \sqrt{(x_i-x_j)\,(x_i+4\sqrt{x_i}-x_j+4)} \qquad x_l = \frac{M^2_{N_l}}{m^2_\eta} \qquad \tilde{\Gamma}_j = \frac{\Gamma_j}{m_\eta}.$$

It should be noted that in the above expression always ($1 \le x_j \le x_i$) where j stands for N_j inside the loop while i stands for N_i as one of the initial state particles, shown in Fig. 1 and in Fig.2. This is simply to realise the "on-shell" -ness of the loop particles in order to generate the required CP asymmetry.

There are several wash-out processes in this scenario, categorised as follows:

- $\Delta L = 2$: $L\eta \to \bar{L}\eta, \eta\eta \to LL$ are purely wash-out processes.
- $\Delta L = 1$: there are two main sources of such wash-out; (i)$N_k \to L\eta$), and (ii) $N_k\eta \to L, X$.

We have taken them into account in our numerical calculations.

Adopting the Casas-Ibarra parametrisation for Yukawa matrix Y, we see that CP phases in U do not contribute to $\varepsilon_{N_i\eta}$, but complex variables in the orthogonal matrix O can lead to non-vanishing value of $\varepsilon_{N_i\eta}$. This is similar to leptogenesis from pure decay in this model [21] where, in the absence of flavour effects, the orthogonal matrix O played a crucial role. In general, this 3×3 orthogonal matrix O can be parameterized by three complex parameters of type $\theta_{\alpha\beta} = \theta^R_{\alpha\beta} + i\theta^I_{\alpha\beta}, \theta^R_{\alpha\beta} \in [0, 2\pi], \theta^I_{\alpha\beta} \in \mathbb{R}$ The above asymmetry along with this rotation (one at a time) takes the following form

$$\varepsilon_{N_i\eta} = \sum_j \frac{(m_j^4-m_i^4)\sin(2\theta^R_{ij})\sinh(2\theta^I_{ij})}{\Lambda_j^2((m_i^2-m_j^2)\cos(2\theta^R_{ij})+(m_i^2+m_j^2)\cosh(2\theta^I_{ij}))}\widetilde{\varepsilon}_{ij}, \tag{3.5}$$

where m_i's are the light neutrino masses and Λ_i's are defined above in Eq. (2.5). On the right hand side of the above equation, a summation over index j is implicit. As an example, we have taken the benchmark values shown in table 1 to compute the baryon asymmetry as well as scalar DM relic numerically. We also take $\theta^R_{23} = \theta^R_{12} = \frac{\pi}{4}\omega, \theta^R_{13} = -\frac{\pi}{4}\omega, \theta^I_{12} = \frac{3\pi}{4}\omega, \theta^I_{13} = \theta^I_{23} = \frac{\pi}{4}\omega$. Here we consider η_I as the DM candidate ($\eta_I \equiv$ DM, corresponding to positive value of quartic coupling λ_5) which is similar to the inert doublet model discussed extensively in the literature [19, 23, 24]. Typically there exists two distinct mass regions, $M_{\rm DM} \le 80$ GeV and $M_{\rm DM} \ge 500$ GeV, where

Parameter	Required parameter for Correct Relic	Particle	Mass
μ_η	870 GeV	m_{η_R}	870 GeV
λ_1	0.253	m_{η_I}	870 GeV
λ_3	0.65	$m_{\eta^\pm}$	881 GeV
λ_4	-0.65	M_{N_1}	1. TeV
λ_5	8×10^{-6}	M_{N_2}	1.5 TeV
λ_2	1	M_{N_3}	2. TeV

Table 1: The numerical values of the parameters chosen for generating correct scalar DM relic and baryon asymmetry. We denote it as benchmark point 1 (BP1). For Normal (Inverted) Hierarchy $\omega = 0.7(0.56)$.

correct relic abundance criteria can be satisfied. In both regions, depending on the mass differences $m_{\eta^\pm} - m_{\eta_I}, m_{\eta_R} - m_{\eta_I}$, the coannihilations of $\eta_I, \eta^\pm$ and η_R, η_I can also contribute to the DM relic abundance [25, 26]. As for the mixing angles in the PMNS matrix U we took the best fit values obtained from the recent global fit analysis [28] shown in the table 2.

θ_{12}	θ_{13}	θ_{23}	$\Delta m^2_{21}\times10^{-5}(\mathrm{eV}^2)$	$\lvert\Delta m^2_{31}\rvert\times10^{-3}(\mathrm{eV}^2)$	$m_{lightest}(\mathrm{eV})$
33.7°	8.8°	41.4°	7.54	2.43	0.01

Table 2: The numerical values of light neutrino parameters used in the calculations.

To perform the numerical analysis, we implement the model in `SARAH 4` [29] and extract the thermally averaged annihilation rates from `micrOMEGAs 4.3` [30] to use while solving the Boltzmann equations above. In Fig. 3, we plot the comoving number densities of all Z_2 odd particles, taking part in generating the lepton asymmetry along with the generated asymmetry ΔL, as functions of temperature. The left panel corresponds to normal hierarchy (NH) of neutrino mass spectrum and the right panel to the case of inverted hierarchy (IH). The horizontal solid black line labelled as "ΔL observed" correspond to the value of ΔL that is partially converted into the observed baryon asymmetry via the electroweak sphaleron processes with the conversion factor $C_s = \frac{8N_f+4N_H}{22N_f+13N_H}$ where $N_f = 3, N_H = 2$ are the number of fermion generations and Higgs doublets respectively [31]. While sphalerons violate $B+L$, they conserve $B-L$ symmetry. The sphaleron processes are effective with a thermal rate $\Gamma_{\rm sph} \sim (\alpha_2 T)^4$ with $SU(2)$ gauge coupling constant α_2 at high temperature until EW phase transition, while they are exponentially suppressed due to finite gauge boson masses after EW gauge symmetry breaking. The shaded regions in the panels correspond to the temperature below which the sphaleron processes become inoperative($T \lesssim 200$ GeV [32]). The benchmark parameters are chosen in such a way that the generated lepton asymmetry ΔL by the epoch of sphaleron freeze-out is sufficient enough to produce the observed baryon asymmetry. The dashed horizontal black line corresponds to the observed DM relic abundance in the present universe [1]. As can be seen from this plot, the lepton asymmetry grows as the temperature cools down due to the contributions from the co-annihilation diagrams. While the lepton asymmetry gets converted into the baryon asymmetry at EW phase transition temperature, it takes a while for DM to freeze-out. Since non-zero CP asymmetry arises from coannihilations between η and heavier right handed neutrinos $N_{2,3}$, the lepton number generating processes get frozen out much earlier compared to DM self annihilations. This makes sure that a net lepton asymmetry is created with the right amount without being washed out entirely. The limits on the parameter λ_5, keeping all the other parameters same as shown on table 1, are set by two constraints. One is the mass difference between the neutral scalar and pseudo-scalar ($\Delta = m_{\eta_R} - m_{\eta_I}$) which needs to be more than approximately 100 keV, in order to avoid Z mediated inelastic direct detection scattering of DM off nucleons, as we discuss below. The other constraint is coming from the required leptonic asymmetry with maximal CP asymmetry. Then, the ranges are $\lambda_5 = (0.3 - 8.1) \times 10^{-5}$ for NH and $\lambda_5 = (0.03 - 1.2) \times 10^{-4}$ for IH.

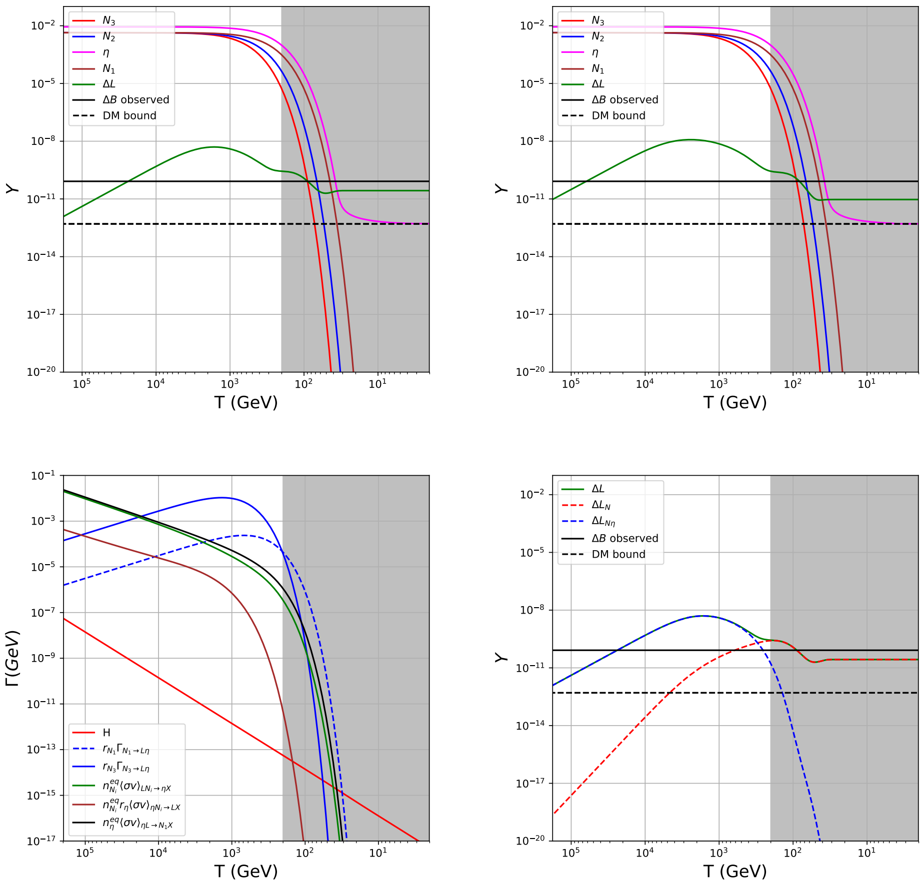

Figure 3: Top panel: comoving number densities of Z_2 odd particles and lepton asymmetry as a function of T for scalar DM scenario. The left (right) panel corresponds to the normal (inverted) hierarchy of neutrino mass spectrum. Bottom panel: rates of individual wash-out processes along with the Hubble rate (left panel); individual (co)annihilation contributions of each channel to the asymmetry. The solid (dashed) black line corresponds to the baryon asymmetry (DM abundance) observed at present epoch ($T \sim 0$). Shaded regions represent the epochs after sphaleron freeze out.

3.2 Right handed neutrino as dark matter

If the lightest Z_2 odd particle is the lightest of the right handed neutrinos (and hence the DM candidate), then the annihilation processes responsible for creating a non-zero lepton asymmetry are shown in Fig. 4. Once again, pure self annihilation of DM can not provide the asymmetry due to the absence of "on-shell" condition for loop particles. If the scalar doublet η is the next to the lightest Z_2 odd particle, then the annihilation processes shown in Fig. 4 can produce the required lepton asymmetry. For this scenario the Boltzmann equations for the Z_2 odd particles take the following form:

$$\begin{aligned}
\frac{dY_{N_k}}{dz} &= -\frac{1}{zH(z)}\Bigg[(Y_{N_k}-Y_{N_k}^{\rm eq})\langle\Gamma_{N_k\to L_\alpha\eta}\rangle+(Y_{N_k}Y_\eta-Y_{N_k}^{\rm eq}Y_\eta^{\rm eq})s\langle\sigma v\rangle_{\eta N_k\to LSM}\\
&\quad+\sum_{l=1}^{3}(Y_{N_k}Y_{N_l}-Y_{N_k}^{\rm eq}Y_{N_l}^{\rm eq})s\langle\sigma v\rangle_{N_lN_k\to {\rm SMSM}}\Bigg],\quad \text{for } k=2,3\\
\frac{dY_\eta}{dz} &= \frac{1}{zH(z)}\Bigg[\sum_{k=2}^{3}(Y_{N_k}-Y_{N_k}^{\rm eq})\langle\Gamma_{N_k\to L_\alpha\eta}\rangle-(Y_\eta-Y_\eta^{\rm eq})\langle\Gamma_{\eta\to L_\alpha N_1}\rangle\\
&\quad-2(Y_\eta^2-(Y_\eta^{\rm eq})^2)s\langle\sigma v\rangle_{\eta\eta\to{\rm SMSM}}-\sum_{m=1}^{3}(Y_{N_m}Y_\eta-Y_{N_m}^{\rm eq}Y_\eta^{\rm eq})s\langle\sigma v\rangle_{\eta N_m\to LSM}\Bigg],\\
\frac{dY_{N_1}}{dz} &= \frac{1}{zH(z)}\Bigg[(Y_\eta-Y_\eta^{\rm eq})\langle\Gamma_{\eta\to L_\alpha N_1}\rangle-(Y_{N_1}Y_\eta-Y_{N_1}^{\rm eq}Y_\eta^{\rm eq})s\langle\sigma v\rangle_{\eta N_1\to LSM}\\
&\quad-\sum_{l=1}^{3}(Y_{N_1}Y_{N_l}-Y_{N_1}^{\rm eq}Y_{N_l}^{\rm eq})s\langle\sigma v\rangle_{N_lN_1\to{\rm SMSM}}\Bigg].
\end{aligned}\tag{3.6}$$

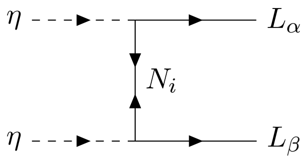

Figure 4: Feynman diagrams of the annihilation processes responsible for creating lepton asymmetry in fermion DM scenario.

Now, in this scenario along with the co-annihilation channels discussed earlier, the annihilation channels shown in Fig. 4 also contribute to the asymmetry. The CP asymmetry coming from the interference of the tree (Fig. 4) and the loop (bottom two diagrams in Fig. 2) leading to $\mathscr{O}(y^6)$ are given as:

$$\begin{aligned}
\varepsilon_{\eta\eta} &= 8\sum_{ij}\left(\Im[(yy^\dagger)_{i1}(yy^\dagger)_{j1}(yy^\dagger)_{ij}]\right)\varepsilon_{ij}^{ann}\\
&= \sum_j\frac{m_1^4-m_j^4}{\Lambda_1^4\Lambda_j^2}\left(\Delta m_{1j}^2\sin(4\theta_{1j}^R)+(m_1^2+m_j^2)\sinh(4\theta_{1j}^I)\right)\varepsilon_{1j}^{ann},\\
\varepsilon_{1j}^{ann} &= 7\frac{1}{16\pi}\left[1-r_1-\frac{1}{2}(r_1-3)\ln\left[\frac{1+r_1}{3-r_1}\right]\right]\frac{\sqrt{r_jr_1}}{(1+r_j)(1+r_1)}\frac{1}{\mathscr{M}_{tree}},
\end{aligned}\tag{3.7}$$

$$\mathscr{M}_{tree} = \sum_{ij}(yy^\dagger)_{ij}^2\frac{\sqrt{r_i}\sqrt{r_j}}{(1+r_i)1+r_j)}.\tag{3.8}$$

At this point one may notice that the asymmetry expression given in Eq.(3.4) is much more complicated than the one given in Eq. (3.7) which is purely due to the presence of several coannihilating

Parameter	Required parameter for Correct Relic
$\mu_\eta = M_{\eta_R} = M_{\eta_I}$	870 GeV
$M_{\eta_\pm}$	876.3 GeV
M_{N_1}	$M_{\eta_\pm} - \Delta m$ GeV
Δm	10 GeV
$M_{N_2} = 1/2 M_{N_3}$	1 TeV
λ_1	0.253
λ_3	1.48
λ_4	-1.48
λ_5	1×10^{-5}
λ_2	1
$-\theta^R_{ij} = \theta^I_{13} = \theta^I_{23}$	$-\frac{\pi}{4}\omega$
θ^I_{12}	$\frac{3\pi}{4}\omega$

Table 3: The numerical values of the parameters chosen for generating correct Fermion DM relic and baryon asymmetry. We denote it as benchmark point 2 (BP2). For Normal (Inverted) Hierarchy $\omega = 0.85(0.45)$.

particles.. As pointed out earlier, in this scenario we would require at least one of the right handed neutrinos to be lighter than the scalar doublet η whose annihilations are responsible for creating the asymmetry. In our case we have considered only N_1 to be lighter than η and the rest to be heavier. Alternatively, if $N_{2,3}$ are lighter than η, then their (co)annihilations can contribute more to the generation to the asymmetry. For our chosen benchmark points, as shown in table 3, the contribution of $N_{2,3}$ annihilations to lepton asymmetry is sub-dominant compared to η annihilations as well as $\eta - N_k$ $(k = 2,3)$ coannihilations. In fact in the fermion DM scenario, both $\eta - N_k$ $(k = 2,3)$ coannihilations (shown in Fig. 1) as well as η annihilations (shown in Fig. 4) can contribute to lepton asymmetry. It is worthwhile to note that the η annihilations shown in Fig. 4 can not contribute to lepton asymmetry in the scalar DM scenario due to the absence of "on-shell" condition for loop particles.

The washout effects in this scenario are categorised as follows :

- $\Delta L = 2$: $\eta\eta \to LL$ and $L\eta \to \overline{L}\eta$.
- $\Delta L = 1$: $N_k \to L\eta$, $\eta \to LN_k$, and $N_k\eta \to L, X(= \gamma, W, h)$

In Fig. 5, we plot the predictions for relic abundance of all Z_2 odd particles, taking part in generating the lepton asymmetry along with the generated asymmetry ΔL, as functions of temperature, for fermion DM scenario. The upper left panel corresponds to the NH of neutrino masses, whereas the upper right panel to the IH of neutrino masses. In the lower panel, we compare the relative contributions to the lepton asymmetry: from $\eta - \eta$ annihilations (ΔL_η), from $\eta - N_k$ coannihilations $(\Delta L_{N\eta})$, from N_2 decay (ΔL_N), as functions of temperature. Similar to the scenario of scalar DM, here also the lepton asymmetry grows as temperature cools due to contributions from the annihilations and coannihilations and saturate around the temperature where the processes responsible for creating the asymmetry tend to go out of equilibrium. Also, the lightest right handed neutrino freezes out to give the required relic abundance for DM in the universe. The shaded regions in the panels correspond to the temperature below which the sphaleron processes become inoperative.

The first bump in the curve for the lepton asymmetry shown in upper panel plots of Fig. 5 arises from the coannihilation diagrams while the decay contribution enters later and further increases the asymmetry at later stages. Here we notice that the mass of the lightest right handed fermion is very close to the Z_2 odd scalar counterparts in order to enhance the coannihilations. This is evident from the bottom panel plot of Fig. 5 which shows the co-annihilation among the lightest N and Z_2 odd scalar components contribute dominantly to lepton asymmetry. Along with that we have an interesting feature of λ_5. The bounds on λ_5, $\lambda_5 = (0.027-8)\times 10^{-5}$ for NH and $\lambda_5 = (0.029-6.7)\times 10^{-5}$ for IH, are set by the requirement of the required leptonic asymmetry needed to explain the observed baryonic asymmetry in the Universe and the lower bound is set by the Lepton flavor violating process $\mathrm{BR}(\mu \to e\gamma) < 4.2\times 10^{-13}$ [33], as we discuss below. Since the dark matter candidate is a fermion singlet in this case, the parameter λ_5 is not constrained by dark matter direct detection.

While there exist some wash-out effects for the coannihilating processes, there is not much of that for the annihilation processes, as the processes are already out of equilibrium when wash-out becomes effective. In this case, large Yukawa couplings are required to achieve successful leptogenesis, which in turn leads to very small λ_5, but yet does not affect fermion DM phenomenology much.

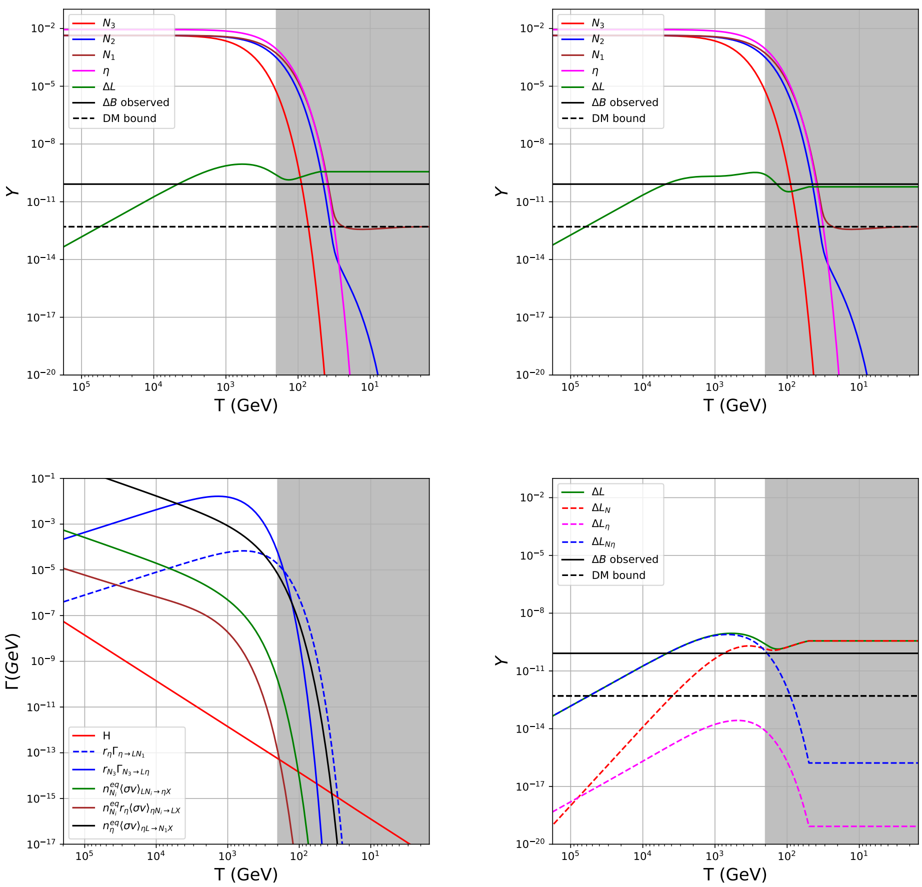

Figure 5: The same as in Fig. 3 but for fermion DM scenario.

We use the `SPheno 3.1` interface to check the constraints from flavour data. We particularly focus on three charged lepton flavour violating (LFV) decays namely, $\mu \to e\gamma, \mu \to 3e$ and $\mu \to e$ (Ti) conversion that have strong current limit as well as good future sensitivity [34]. The present bounds are: $\mathrm{BR}(\mu \to e\gamma) < 4.2 \times 10^{-13}$ [33], $\mathrm{BR}(\mu \to 3e) < 1.0 \times 10^{-12}$ [35], $\mathrm{CR}(\mu, \mathrm{Ti} \to \mathrm{e}, \mathrm{Ti}) < 4.3 \times 10^{-12}$ [36]. While the future sensitivity of the first two processes are around one order of magnitude lower than the present branching ratios, the μ to e conversion (Ti) sensitivity is supposed to increase by six order of magnitudes [34] making it a highly promising test to confirm or rule out different TeV scale BSM scenarios. It should be noted that such charged LFV process arises in the SM at one loop level and remains suppressed by the smallness of neutrino masses, much beyond the current and near future experimental sensitivities. Therefore, any experimental observation of such processes is definitely a sign of BSM physics, like the one we are studying here. We show the predictions for LFV processes in our model in Fig. 6, also highlighting the second benchmark point (BP2) mentioned above. The similar contributions for the BP1 scenario remain far more suppressed due to smallness of the corresponding Yukawa couplings. The scatter plot in Fig. 6 is obtained by only varying μ_η from 100 GeV to 1 TeV, and fixing the other parameters with the values presented in table 3. It can be seen that some part of the parameter space, specially the region which generates correct DM abundance, lies close to the current experimental limits. As mentioned earlier, this bound on $\mathrm{BR}(\mu \to e\gamma)$ decides the lower bound on the parameter λ_5. If λ_5 is lower than the one chosen in BP2, the corresponding Yukawa couplings will be bigger (from Casas-Ibarra parameterisation) enhancing the decay rate. For $\mu \to e\gamma$, the latest MEG 2016 limit [33] can already rule out several points. The promising future sensitivity of the μ to e conversion (Ti) will be able to explore most part of the parameter space.

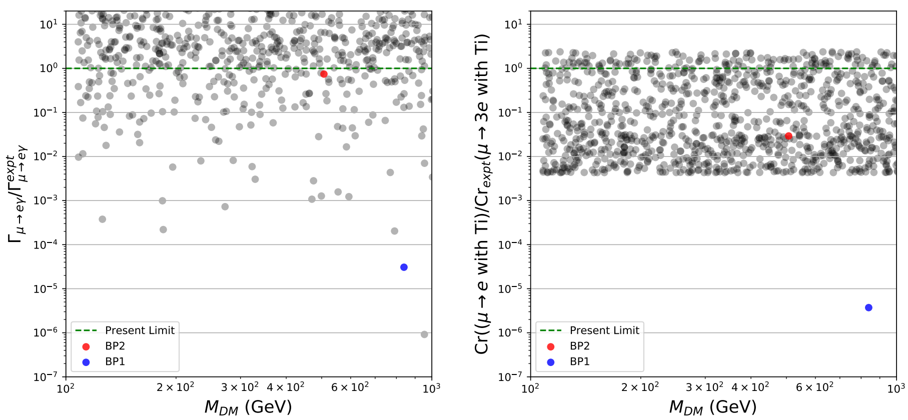

Figure 6: Predictions for LFV processes for 10^2 GeV $< M_{\mathrm{DM}} < 10^3$ GeV. The two benchmark points are highlighted with red and blue coloured points. The μ_η are varied from 100 GeV to 1 TeV, and the other parameters are taken as presented in table 3.

4. Conclusion

We have proposed a scenario where baryogenesis via leptogenesis can be achieved through annihilations and coannihilations of particles belonging to a Z_2 odd sector including t-channel processes. We have considered a popular model known as the scotogenic model to implement the idea, and addressed the the possibility of explaining the coincidence of DM abundance and baryon asymmetry in the present universe along with non-zero neutrino masses. Pointing out two different possible scenarios corresponding to scalar and fermion DM respectively, we show the non-trivial role played by t-channel annihilation as well as coannihilation processes between different Z_2 odd particles. Another interesting feature is the testability of the model at DM direct detection and rare decay experiments. Even though the particle spectrum is in a few $\mathcal{O}(100)$ GeV regime or above, away from the reach of current collider experiments, the model can still be tested at near future run of rare decay experiments looking for charged lepton flavour violation like $\mu \to e\gamma, \mu \to 3e$, μ to e conversion etc.

Acknowledgments

One of the authors, DB acknowledges the hospitality and facilities provided by School of Liberal Arts, Seoul-Tech, Korea where this work was completed. SK and AD were supported by the National Research Foundation of Korea (NRF) grants (2017K1A3A7A09016430, 2017R1A2B4006338).

References

[1] **Planck** Collaboration, N. Aghanim et al., *Planck 2018 results. VI. Cosmological parameters*, arXiv:1807.06209.

[2] S. Weinberg, *Cosmological Production of Baryons*, *Phys. Rev. Lett.* **42** (1979) 850–853.

[3] E. W. Kolb and S. Wolfram, *Baryon Number Generation in the Early Universe*, *Nucl. Phys.* **B172** (1980) 224. [Erratum: Nucl. Phys.B195,542(1982)].

[4] M. Fukugita and T. Yanagida, *Baryogenesis Without Grand Unification*, *Phys. Lett.* **B174** (1986) 45–47.

[5] **Particle Data Group** Collaboration, C. Patrignani et al., *Review of Particle Physics*, *Chin. Phys.* **C40** (2016), no. 10 100001.

[6] S. Nussinov, *TECHNOCOSMOLOGY: COULD A TECHNIBARYON EXCESS PROVIDE A 'NATURAL' MISSING MASS CANDIDATE?*, *Phys. Lett.* **165B** (1985) 55–58.

[7] H. Davoudiasl and R. N. Mohapatra, *On Relating the Genesis of Cosmic Baryons and Dark Matter*, *New J. Phys.* **14** (2012) 095011, [arXiv:1203.1247].

[8] K. Petraki and R. R. Volkas, *Review of asymmetric dark matter*, *Int. J. Mod. Phys.* **A28** (2013) 1330028, [arXiv:1305.4939].

[9] K. M. Zurek, *Asymmetric Dark Matter: Theories, Signatures, and Constraints*, *Phys. Rept.* **537** (2014) 91–121, [arXiv:1308.0338].

[10] M. Yoshimura, *Unified Gauge Theories and the Baryon Number of the Universe*, *Phys. Rev. Lett.* **41** (1978) 281–284. [Erratum: Phys. Rev. Lett.42,746(1979)].

[11] S. M. Barr, *Comments on Unitarity and the Possible Origins of the Baryon Asymmetry of the Universe*, *Phys. Rev.* **D19** (1979) 3803.

[12] I. Baldes, N. F. Bell, K. Petraki, and R. R. Volkas, *Particle-antiparticle asymmetries from annihilations*, *Phys. Rev. Lett.* **113** (2014), no. 18 181601, [arXiv:1407.4566].

[13] Y. Cui, L. Randall, and B. Shuve, *A WIMPy Baryogenesis Miracle*, *JHEP* **04** (2012) 075, [arXiv:1112.2704].

[14] N. Bernal, F.-X. Josse-Michaux, and L. Ubaldi, *Phenomenology of WIMPy baryogenesis models*, *JCAP* **1301** (2013) 034, [arXiv:1210.0094].

[15] N. Bernal, S. Colucci, F.-X. Josse-Michaux, J. Racker, and L. Ubaldi, *On baryogenesis from dark matter annihilation*, *JCAP* **1310** (2013) 035, [arXiv:1307.6878].

[16] J. Kumar and P. Stengel, *WIMPy Leptogenesis With Absorptive Final State Interactions*, *Phys. Rev.* **D89** (2014), no. 5 055016, [arXiv:1309.1145].

[17] J. Racker and N. Rius, *Helicitogenesis: WIMPy baryogenesis with sterile neutrinos and other realizations*, *JHEP* **11** (2014) 163, [arXiv:1406.6105].

[18] A. Dasgupta, C. Hati, S. Patra, and U. Sarkar, *A minimal model of TeV scale WIMPy leptogenesis*, arXiv:1605.01292.

[19] E. Ma, *Verifiable radiative seesaw mechanism of neutrino mass and dark matter*, *Phys. Rev.* **D73** (2006) 077301, [hep-ph/0601225].

[20] J. Racker, JCAP **1403**, 025 (2014) doi:10.1088/1475-7516/2014/03/025 [arXiv:1308.1840 [hep-ph]].

[21] T. Hugle, M. Platscher, and K. Schmitz, *Low-Scale Leptogenesis in the Scotogenic Neutrino Mass Model*, arXiv:1804.09660.

[22] J. A. Casas and A. Ibarra, *Oscillating neutrinos and muon $\to$ e, gamma*, *Nucl. Phys.* **B618** (2001) 171–204, [hep-ph/0103065].

[23] R. Barbieri, L. J. Hall, and V. S. Rychkov, *Improved naturalness with a heavy Higgs: An Alternative road to LHC physics*, *Phys. Rev.* **D74** (2006) 015007, [hep-ph/0603188].

[24] L. Lopez Honorez, E. Nezri, J. F. Oliver, and M. H. G. Tytgat, *The Inert Doublet Model: An Archetype for Dark Matter*, *JCAP* **0702** (2007) 028, [hep-ph/0612275].

[25] K. Griest and D. Seckel, *Three exceptions in the calculation of relic abundances*, *Phys. Rev.* **D43** (1991) 3191–3203.

[26] J. Edsjo and P. Gondolo, *Neutralino relic density including coannihilations*, *Phys. Rev.* **D56** (1997) 1879–1894, [hep-ph/9704361].

[27] D. Borah, A. Dasgupta and S. K. Kang, PoS ICHEP **2018**, 929 (2019) doi:10.22323/1.340.0929 [arXiv:1811.02094 [hep-ph]]; D. Borah, A. Dasgupta and S. K. Kang, arXiv:1806.04689 [hep-ph].

[28] I. Esteban, M. C. Gonzalez-Garcia, A. Hernandez-Cabezudo, M. Maltoni and T. Schwetz, arXiv:1811.05487 [hep-ph].

[29] F. Staub, *SARAH 4 : A tool for (not only SUSY) model builders*, *Comput. Phys. Commun.* **185** (2014) 1773–1790, [arXiv:1309.7223].

[30] D. Barducci, G. Belanger, J. Bernon, F. Boudjema, J. Da Silva, S. Kraml, U. Laa, and A. Pukhov, *Collider limits on new physics within micrOMEGAs 4.3*, *Comput. Phys. Commun.* **222** (2018) 327–338, [arXiv:1606.03834].

[31] V. A. Kuzmin, V. A. Rubakov and M. E. Shaposhnikov, Phys. Lett. **155B**, 36 (1985).

[32] M. D'Onofrio, K. Rummukainen and A. Tranberg, Phys. Rev. Lett. **113**, no. 14, 141602 (2014) doi:10.1103/PhysRevLett.113.141602 [arXiv:1404.3565 [hep-ph]].

[33] **MEG** Collaboration, A. M. Baldini et al., *Search for the lepton flavour violating decay $\mu^+ \to e^+\gamma$ with the full dataset of the MEG experiment*, *Eur. Phys. J.* **C76** (2016), no. 8 434, [arXiv:1605.05081].

[34] T. Toma and A. Vicente, *Lepton Flavor Violation in the Scotogenic Model*, *JHEP* **01** (2014) 160, [arXiv:1312.2840].

[35] **SINDRUM** Collaboration, U. Bellgardt et al., *Search for the Decay $\mu^+ \to e^+e^+e^-$* , *Nucl. Phys.* **B299** (1988) 1–6.

[36] **SINDRUM II** Collaboration, C. Dohmen et al., *Test of lepton flavor conservation in $\mu \to e$ conversion on titanium*, *Phys. Lett.* **B317** (1993) 631–636.